Nanopillar Arrays

DOI: 10.1002/anie.200801335

Periodic Positioning of Multilayered [2.2]Paracyclophane-Based Nanopillars**

David Bléger, David Kreher, Fabrice Mathevet, André-Jean Attias, Imad Arfaoui, Germain Metgé, Ludovic Douillard, Céline Fiorini-Debuisschert, and Fabrice Charra**

The development of conjugated organic molecules as building blocks capable of ordering on well-defined surfaces is an active research area in view of future applications in molecular electronics,[1] photonics,[2] and nanomechanical devices.[3,4] Bottom-up approaches based on supramolecular chemistry are of particular interest for formation of preprogrammed organic self-assembled monolayers.[5] Extensive efforts have been concentrated, independently, in two directions. The first, based on upright-oriented chemisorbed molecules such as thiols, consists of stacking functional moieties in the off-plane direction,[6] which is usually detrimental for lateral order. The second, the objective of which is the mastering of increasingly complex lateral organizations, is based on two-dimensional molecules forming essentially planar structures.[7] Combining complex in-plane self-organizations and off-plane protrusions in self-assembled molecular architectures is an important current challenge.[8] This is a key requirement, for example, for the realization of biological molecular receptors[6] or for decoupling electronically active molecules from a conducting substrate.[9] The latter is currently achieved either through insulating layers[10] or by introduction of molecular spacer units.[11] However, such modifications strongly perturb the lateral organization. Moreover, complex combinations of in-plane and off-plane structures are precluded. A first step towards such combinations is the nanoscale positioning of rigid upstanding elements.

We recently proposed a strategy to form "on-demand" noncovalent self-assemblies with predetermined 2D topologies on highly oriented pyrolitic graphite (HOPG) at the liquid/solid interface at room temperature.[12] This method is based on a novel functional unit which acts as a cliplike noncovalent bond on HOPG. Here, we exploit this approach for the realization of 2D patterns of well-defined 3D nanostructures.

Our strategy follows classical architectural paradigms based on the realization of a well-organized in-plane monolayer on HOPG and the emergence, perpendicular to the substrate, of a periodic array of standing organic nanopillars of tunable height. To validate this concept, we chose the multilayered [2.2]paracyclophane (PCP) moiety as a nanopillar of variable height. More precisely, we designed and synthesized a series of compounds (Scheme 1) bearing two functional "clips"[12] that end-cap a central benzene ring (**I**) or the lower deck of two- and three-layered PCP units (**II** and **III**, respectively). Thus, bifunctional building blocks **I**–**III** can be considered to be one-, two-, and three-storied compounds. Here we demonstrate that all these multistory compounds are able to self-assemble as linear chains,[12] whereby **II** and **III** build up perpendicular to the HOPG substrate. Moreover, to elucidate the role of the common base of **II** and **III** in the formation of linear chains, **I** was designed as a model compound with two lateral methyl substituents on the central ring to mimic the steric hindrance of the [2.2]paracyclophane units in **II** and **III**. The synthetic routes to **I**–**III** are outlined in Scheme 2.

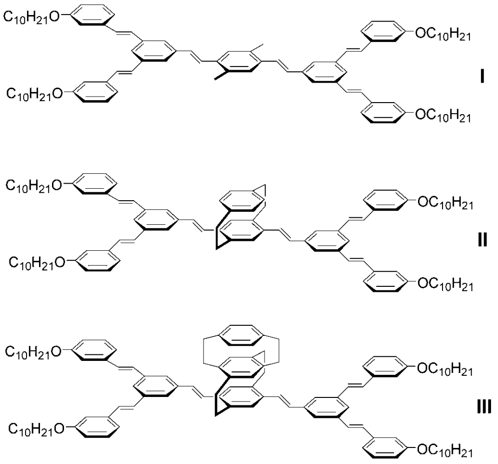

Scheme 1. Molecular structures of one-, two-, and three-layered [2.2]paracyclophane-based compounds **I**–**III**. Only one of the two enantiomers of **II** is shown, and for **III** only one of the four stereoisomers relative to the central cyclophane is represented (see Supporting Information).

---

[*] D. Bléger, Dr. D. Kreher, Dr. F. Mathevet, Prof. A.-J. Attias
Laboratoire de Chimie des Polymères-UMR 7610
Université Pierre et Marie Curie
4 place Jussieu – case 185, 75252 Paris CEDEX 05 (France)
Fax: (+33) 1-4427-7089
E-mail: andre-jean.attias@upmc.fr
Homepage: http://www.lcp.upmc.fr

Dr. I. Arfaoui, G. Metgé, Dr. L. Douillard, Dr. C. Fiorini-Debuisschert, Dr. F. Charra
CEA, IRAMIS, Service de Physique et Chimie des Surfaces et Interfaces, Lab. de Nanophotonique
91191, Gif-sur-Yvette CEDEX (France)
E-mail: fabrice.charra@cea.fr
Homepage: http://iramis.cea.fr

[**] This work has been supported by the Région Ile-de-France in the framework of C'Nano-IdF. C'Nano-IdF is the nanoscience competence center of Paris Region, supported by CNRS, CEA, MESR, and Région Ile-de-France.

Supporting information for this article is available on the WWW under http://dx.doi.org/10.1002/anie.200801335.

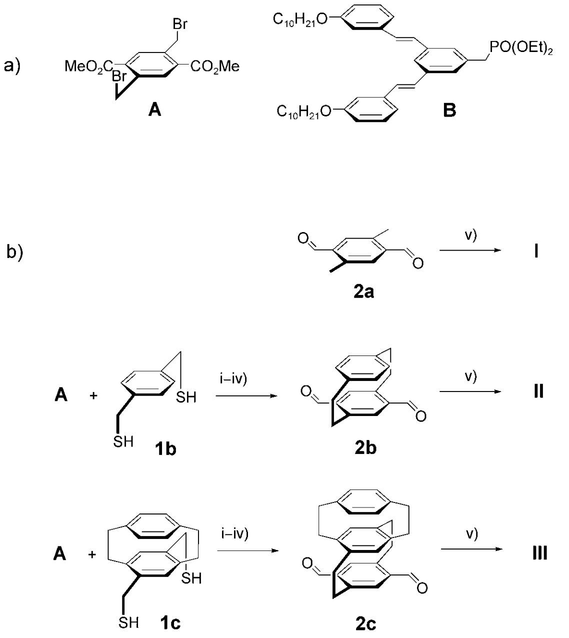

Scheme 2. a) Chemical structure of key compound **A** and "clip" **B**. b) Synthesis of **I**–**III**. i) KOH, MeOH, CH_2Cl_2, RT, 5 h; ii) $P(OEt)_3$, $h\nu$, 6 h; iii) $LiAlH_4$, THF, reflux, 6 h; iv) Pyridinium chlorochromate (PCC), CH_2Cl_2, RT, 2 h; v) *t*BuOK, THF, **B**, RT, 1 h.

Pillars **2b** and **2c** were obtained by adaptation of standard procedures.[13,14] Then **2a**,[15] **2b**, and **2c** were treated with clip phosphonate derivative **B**[12] to give the planar one-layered target (**I**) and two- (**II**) and three-layered (**III**) 3D compounds. On the basis of X-ray crystallographic analysis of multilayered [2.2]paracyclophane,[16] we assume that clip functionalized nanopillars **II** and **III** have heights of 3.0 and 6.0 Å, respectively.

Self-assembly of **I**–**III** was studied by scanning tunneling microscopy (STM) on HOPG at the solid/liquid interface at room temperature. Figure 1 shows the STM image of pedestal molecules **I**. The bright four-branched patterns can be attributed to the rigid conjugated cores (yellow in the superimposed to-scale model). The experimental lattice parameters are $a = (3.86 \pm 0.15)$ nm, $b = (2.11 \pm 0.08)$ nm, and $\alpha = 65 \pm 1°$ (red arrows in Figure 1).

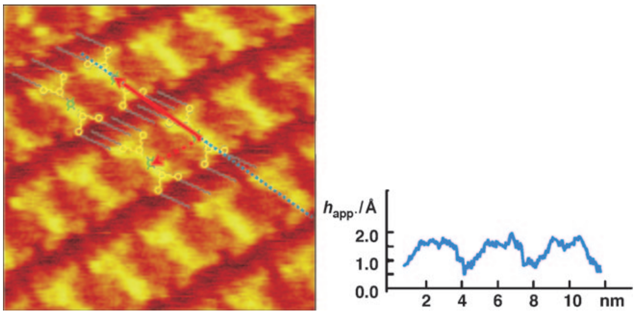

Figure 1. Self-assembly of planar model compound **I**. High-resolution STM image of a monolayer of **I** formed at the interface between HOPG and an approximately 10^{-4} mol L^{-1} solution. The sample bias was −1.55 V, and the tunnel current 55 pA. The scan size and *Z* scale were 12.5 nm and 2.0 Å, respectively. The to-scale model of the molecular assembly with $a = 3.86$ nm, $b = 2.11$ nm, and $\alpha = 65°$ is superimposed. The cross section indicative of the apparent height $h_{app.}$ along the blue dotted line is plotted on the right.

The STM images of self-assembled two- and three-layered PCP-based compounds **II** and **III** are shown in Figure 2. Although the images of the conjugated cores are strongly modified compared to planar **I**, careful inspection of the STM images shows that the underlying conjugated core is still visible, especially for two-layered **II** (Figure 2a). The cyclophane multistory system appears as a central bright round spot. This spot is wider for the three-story compound **III**, and thus it smears the image of the base. Apart from a lattice fault in the central part of Figure 2a (discussed below), the cell parameters are unaltered compared to model system **I**. The lattice fault can be interpreted as a juxtaposition variant of neighboring clipped-molecule chains and thus confirms the clipping direction and the role of independent structural entities of these chains, despite the presence of a multilayered PCP moiety.

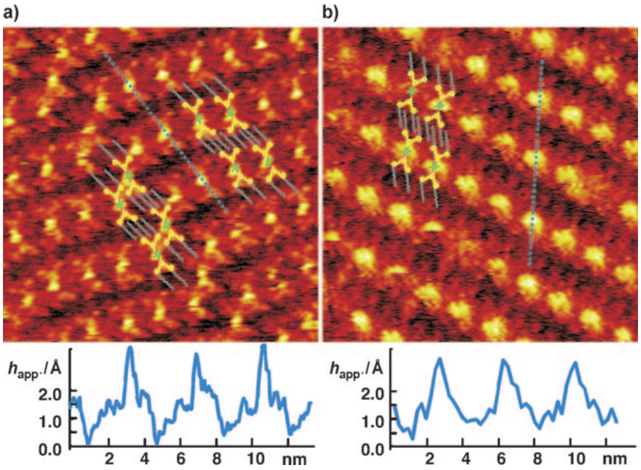

Figure 2. Self-assembly of multilayered PCP-based compounds **II** and **III**. STM image of a monolayer of a) two-layered compound **II** (sample bias −0.95 V, tunnel current 12 pA, scan size 20.5 nm, solution concentration 10^{-2} mol L^{-1}) and b) three-layered compound **III** (sample bias +0.60 V, tunnel current 14 pA, scan size 19.0 nm, solution concentration 10^{-4} mol L^{-1}) formed at the interface between HOPG and solution. The scaled models of the molecular assembly are superimposed on each STM image. The cross sections indicative of the apparent height along the blue dotted lines are plotted below each STM images (same scale as in Figure 1).

Regarding the off-plane protrusions, apparent-height cross-sections of both **II** and **III** (see Figure 2) show alternating peaks and valleys with period $a = (3.86 \pm 0.15)$ nm. For two-layered **II**, the apparent height of the cyclophane moiety is about twice the apparent height of the conjugated part of the pedestal, which appears as shoulders at the base of the cyclophane peaks. For three-layered **III** the simple additive rule breaks down for spectroscopic reasons, since the optimum imaging bias is strongly altered compared to the planar and two-layered systems.[17]

A more detailed analysis of the STM images permits the epitaxial relationship with respect to the HOPG lattice to be identified. As shown in Figure 3 a, two families of mirror-symmetric domains are observed. By symmetry, each left- or right-handed domain must form an angle of $+\theta$ or $-\theta$ (mod 60°) with a symmetry axis of HOPG. From experimental data we obtained $\theta = 50° \pm 1°$ (mod 60°) for the a axis of left-handed domains (labeled (L) in Figure 3 a, where $\theta = 49°$). A unit cell that is a multiple of the HOPG atomic lattice and best matches the experimental data is shown in Figure 3 b (red arrows). It corresponds to a super lattice $\begin{pmatrix} 14 & 1 \\ 3 & 8 \end{pmatrix}$ with $a = 3.84$ nm, $b = 2.08$ nm, $\alpha = 63.9°$, and $\theta = \pm 50.4°$, in agreement with experimental data. From the positions of the imaged conjugated cores relative to this lattice and the direction of the clips inferred from the lattice faults (Figure 2 a), the molecular organization shown in Figure 3 b can be determined. Superimposition of this model on the STM images in Figure 1 and Figure 2 a,b shows the agreement between the positions of the conjugated moieties in the model and the experimental observations. Note that the left-handed model in Figure 3 b contains one molecule per unit cell and is based on a given enantiomer of **II** or **III**. Both enantiomers must thus segregate within domains of opposite orientation. The stacking fault in Figure 2 a corresponds to sliding of the clipped molecular chains along the direction of the alkyl chains, as indicated in Figure 3 b (blue arrows). This shift increases the coverage by **II** at the expense of reduced interactions between alkyl chains, consistent with its occurrence at higher concentration.

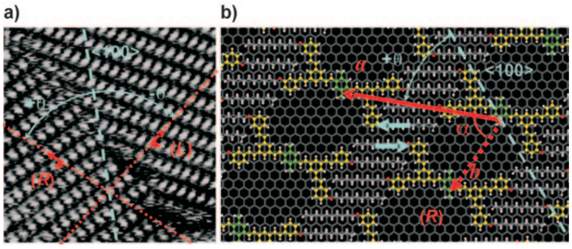

Figure 3. Molecular model of adsorption on HOPG. a) An STM image showing two domains of opposite chiral orientations labeled (R) and (L) for **II** (sample bias −1.0 V, tunnel current 9 pA, scan size 33 nm, Z scale 3.0 Å). The unit cells are represented by red arrows. Their a axes form an angle $\pm\theta$ from a symmetry axis of HOPG (in blue, here $\theta = 50° \pm 1°$). b) Molecular scheme of one unit cell of the monolayer adsorbed on HOPG (background gray honeycomb). Gray: alkyl chains; yellow: conjugated cores, green: PCP moiety. The unit cell is represented by red arrows: the solid arrow represents the intrachain period, and the dotted arrow the interchain period. The blue line represents one ⟨100⟩ axis of HOPG. The blue arrows show the interchain sliding direction parallel to alkyl chains and another ⟨100⟩ axis.

Notably, single domains of molecules of any one of **I**, **II**, or **III** may extend over large distances, as demonstrated in the STM image of Figure 4, acquired by using a low-concentration (10^{-4} mol L^{-1}) solution in order to eliminate stacking faults. The coherence remains on high-curvature substrates, as shown over the diagonal substrate default, which correspond to radii of surface curvature as small as 150 nm. This shows the high tolerance of the self-assembly process with respect to geometrical constraints possibly imposed by the topmost graphene layer.

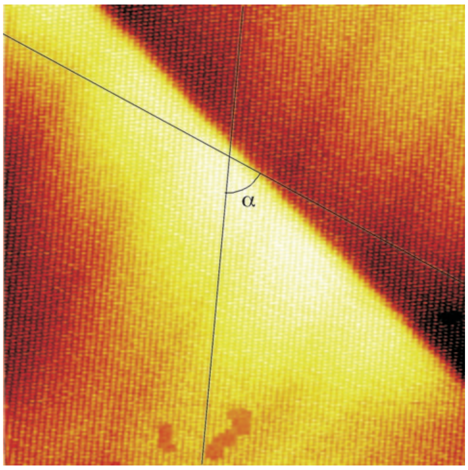

Figure 4. Long-range organization of two-layered PCP-based compound **II**. Large-scale (255 × 255 nm) STM image of a monolayer single domain of **II** formed at the interface between HOPG and a highly diluted solution (ca. 10^{-4} mol L^{-1}), including a near-surface buried dislocation of graphite (sample bias −0.65 V, tunnel current 16 pA, Z scale 6.0 Å). The experimental lattice parameters are indicated, and the corresponding straight lines show the strict coherence of the domain over the whole scanned area, including the high-curvature regions.

In summary, we have established a simple general strategy for controlled 3D nanopatterning of HOPG at the liquid/solid interface at room temperature. End-capping, by a convergent synthetic route, of the lower deck of pillarlike structures with a molecular clip specifically designed to promote organization on HOPG leads to building blocks whose controlled in-plane self-assembly allows the positioning of vertical structural elements in large unit cells. The versatile approach presented here, combined with further convenient functionalization of the upper deck of the pillar, could provide a promising route for inserting 3D functional nanostructures into 2D lattices en route to supramolecular devices.

Experimental Section

Procedures for the synthesis of **I–III** are available in the Supporting Information.

STM images were acquired at room temperature with a home-made digital system. The images reported here were obtained in the current mode, with slow height regulation. The fast scan axis was kept perpendicular to the sample slope. Images acquired simultaneously in both fast scan directions are systematically recorded and compared. All images are corrected for the drift of the instrument by combining two successive images with downward and upward slow-scan directions.

The solvent was phenyloctane (Aldrich, 98 %), which avoids the coadsorbtion often observed with linear alkanes. The substrate was HOPG (Goodfellow) and the tips were mechanically formed from a 250-mm Pt/Ir wire (Pt80/Ir20, Goodfellow). The monolayers were formed by immersing the STM junction in a droplet (ca. 10 mL) of solution immediately after cleaving the substrate and approaching the STM tip.

Received: March 19, 2008
Revised: July 8, 2008

Keywords: cyclophanes · nanostructures · scanning probe microscopy · self-assembly · surface functionalization

[1] C. Joachim, J. K. Gimzewski, A. Aviram, *Nature* **2000**, *408*, 541.

[2] H. Imahori, *Bull. Chem. Soc. Jpn.* **2007**, *80*, 621.

[3] R. A. van Delden, M. K. J. ter Wiel, M. M. Pollard, J. Vicario, N. Koumura, B. L. Feringa, *Nature* **2005**, *437*, 1337.

[4] Y. Liu, A. H. Flood, P. A. Bonvallett, S. A. Vignon, B. H. Northrop, H. R. Tseng, J. O. Jeppesen, T. J. Huang, B. Brough, M. Baller, S. Magonov, S. D. Solares, W. A. Goddard, C. M. Ho, J. F. Stoddart, *J. Am. Chem. Soc.* **2005**, *127*, 9745.

[5] a) J. V. Barth, G. Costantini, K. Kern, *Nature* **2005**, *437*, 671; b) J. V. Barth, *Annu. Rev. Phys. Chem.* **2007**, *58*, 375; c) S. De Feyter, F. C. De Schryver, *Chem. Soc. Rev.* **2003**, *32*, 139; d) M. Surin, P. Samori, *Small* **2007**, *3*, 190; e) P. Samorì, *J. Mater. Chem.* **2004**, *14*, 1353; f) F. Rosei, M. Schunack, Y. Naitoh, P. Jiang, A. Gourdon, E. Laegsgaard, I. Stensgaard, C. Joachim, F. Besenbacher, *Prog. Surf. Sci.* **2003**, *71*, 95.

[6] a) F. Schreiber, *Prog. Surf. Sci.* **2000**, *65*, 151; b) J. Huskens, *Curr. Opin. Chem. Biol.* **2006**, *10*, 537; c) N. Miyashitaa, D. G. Kurth, *J. Mater. Chem.* **2008**, *18*, 2636.

[7] a) T. Yokoyama, S. Yokoyama, T. Kamikado, Y. Okuno, S. Mashiko, *Nature* **2001**, *413*, 619; b) J. A. Theobald, N. S. Oxtoby, M. A. Phillips, N. R. Champness, P. H. Beton, *Nature* **2003**, *424*, 1029; c) G. Pawin, K. L. Wong, K. Y. Kwon, L. A. Bartels, *Science* **2006**, *313*, 961; d) S. Weigelt, C. Busse, C. Bombis, M. M. Knudsen, K. V. Gothelf, T. Strunskus, C. Wöll, M. Dahlbom, B. Hammer, E. Laegsgaard, F. Besenbacher, T. R. Linderoth, *Angew. Chem.* **2007**, *119*, 9387; *Angew. Chem. Int. Ed.* **2007**, *46*, 9227; e) L. Grill, M. Dyer, L. Lafferentz, M. Persson, M. V. Peters, S. Hecht, *Nat. Nanotechnol.* **2007**, *2*, 687; f) A. Langner, S. L. Tait, N. Lin, C. Rajadurai, M. Ruben, K. Kern, *Proc. Natl. Acad. Sci. USA* **2007**, *104*, 17927; g) M. Surin, P. Samorì, A. Jouaiti, N. Kyritsakas, M. W. Hosseini, *Angew. Chem.* **2007**, *119*, 249; *Angew. Chem. Int. Ed.* **2007**, *46*, 245; h) P. Samori, A. Fechtenkotter, E. Reuther, M. D. Watson, N. Severin, K. Müllen, J. P. Rabe, *Adv. Mater.* **2006**, *18*, 1317; i) D. Bonifazi, H. Spillmann, A. Kiebele, M. de Wild, P. Seiler, F. Y. Cheng, H. J. Güntherodt, T. Jung, F. Diederich, *Angew. Chem.* **2004**, *116*, 4863; *Angew. Chem. Int. Ed.* **2004**, *43*, 4759; j) S. Furukawa, K. Tahara, F. C. De Schryver, M. Van der Auweraer, Y. Tobe, S. De Feyter, *Angew. Chem.* **2007**, *119*, 2889; *Angew. Chem. Int. Ed.* **2007**, *46*, 2831; k) K. W. Hipps, L. Scudiero, D. E. Barlow, M. P. Cooke, *J. Am. Chem. Soc.* **2002**, *124*, 2126; l) K. G. Nath, O. Ivasenko, J. A. Miwa, H. Dang, J. D. Wuest, A. Nanci, D. F. Perepichka, F. Rosei, *J. Am. Chem. Soc.* **2006**, *128*, 4212; m) K. G. Nath, O. Ivasenko, J. M. MacLeod, J. A. Miwa, J. D. Wuest, A. Nanci, D. F. Perepichka, F. Rosei, *J. Phys. Chem. C* **2007**, *111*, 16996; n) G. Schull, L. Douillard, C. Fiorini-Debuisschert, F. Charra, F. Mathevet, D. Kreher, A. J. Attias, *Nano Lett.* **2006**, *6*, 1360; o) G. Schull, L. Douillard, C. Fiorini-Debuisschert, F. Charra, F. Mathevet, D. Kreher, A. J. Attias, *Adv. Mater.* **2006**, *18*, 2954.

[8] S. Vazquez-Campos, M. Peter, M. Dong, S. Xu, W. Xu, H. Gersen, T. R. Linderoth, H. Schönherr, F. Besenbacher, M. Crego-Calama, D. N. Reinhoudt, *Langmuir* **2007**, *23*, 10294.

[9] a) D. L. Mills, J. X. Cao, R. Q. Wu, *Phys. Rev. B* **2007**, *75*, 205439; b) J. Repp, G. Meyer, S. M. Stojkovic, A. Gourdon, C. Joachim, *Phys. Rev. Lett.* **2005**, *94*, 026803.

[10] a) H. Rauscher, T. A. Jung, J. L. Lin, A. Kirakosian, F. J. Himpsel, U. Rohr, K. Müllen, *Chem. Phys. Lett.* **1999**, *303*, 363; b) X. H. Qiu, G. V. Nazin, W. Ho, *Science* **2003**, *299*, 542; c) N. Ogawa, G. Mikaelian, W. Ho, *Phys. Rev. Lett.* **2007**, *98*, 166103; d) C. J. Villagomez, T. Zambelli, S. Gauthier, A. Gourdon, C. Barthes, S. Stojkovic, C. Joachim, *Chem. Phys. Lett.* **2007**, *450*, 107.

[11] a) R. Otero, Y. Naitoh, F. Rosei, P. Jiang, P. Thostrup, A. Gourdon, E. Laegsgaard, I. Stensgaard, C. Joachim, F. Besenbacher, *Angew. Chem.* **2004**, *116*, 2144; *Angew. Chem. Int. Ed.* **2004**, *43*, 2092; b) M. J. Comstock, N. Levy, A. Kirakosian, J. W. Cho, F. Lauterwasser, J. H. Harvey, D. A. Strubbe, J. M. J. Frechet, D. Trauner, S. G. Louie, M. F. Crommie, *Phys. Rev. Lett.* **2007**, *99*, 038301.

[12] D. Bléger, D. Kreher, F. Mathevet, A. J. Attias, G. Schull, A. Huard, L. Douillard, C. Fiorini-Debuischert, F. Charra, *Angew. Chem.* **2007**, *119*, 7548; *Angew. Chem. Int. Ed.* **2007**, *46*, 7404.

[13] R. Gray, V. Boekelheide, *J. Am. Chem. Soc.* **1979**, *101*, 2128.

[14] N. Kannen, T. Otsubo, Y. Sakata, S. Misumi, *Bull. Chem. Soc. Jpn.* **1976**, *49*, 3307.

[15] J. N. Moorthy, P. Venkatakrishnan, P. Mal, P. Venugopalan, *J. Org. Chem.* **2003**, *68*, 327.

[16] T. Otsubo, S. Mizogami, I. Otsubo, Z. Tozuka, A. Sakagami, Y. Sakata, S. Misumi, *Bull. Chem. Soc. Jpn.* **1973**, *46*, 3519.

[17] Such effects can be explained by differences in the electrostatic influences of tip and substrate potentials experienced by molecular moieties located at different heights from the substrate. For example, see C. Krzeminski, C. Delerue, G. Allan, D. Vuillaume, R. M. Metzger, *Phys. Rev. B* **2001**, *64*, 085405.